

## JHK PHOTOMETRY OF COMPACT PLANETARY NEBULAE

M. Peña and S. Torres-Peimbert

Instituto de Astronomía  
Universidad Nacional Autónoma de México

RESUMEN. Presentamos fotometría infrarroja de 31 nebulosas planetarias compactas. Se encuentra una correlación entre el índice  $(J-H)_0$  y la abundancia de  $\text{He}^+$ . La mayoría de las nebulosas de alta densidad muestran exceso infrarrojo en  $H$  y  $K$  demostrando que poseen polvo más caliente que las nebulosas de menor densidad.

ABSTRACT. We present near infrared photometry of 31 compact planetary nebulae. A correlation of  $(J-H)_0$  with  $\text{He}^+$  abundance is found. Most high density nebulae show infrared excess in  $H$  and  $K$  showing that they have warmer dust than lower density nebulae.

Key words: INFRARED-PHOTOMETRY — NEBULAE-PLANETARY

## I. INTRODUCTION

The study of young planetary nebulae can provide information about the ejection process of the nebular material as well as on nebular evolution and the enrichment of the interstellar medium. The youngest planetary nebulae are expected to be compact and very dense; they usually show signs of variability and IR excess due to the presence of dust which in some cases seems to be mixed with the ionized gas.

Neutral and molecular envelopes outside of the ionized regions have been detected in several of the densest planetary nebulae (e.g., IC 4997, NGC 6302, NGC 6790, Vy 2-2, BD+30°3639, NGC 7027; see Rodríguez 1987 and references therein). Moreover spectral features of dust have been observed in the near IR in several compact PN (Aitken and Roche 1982).

Broad band infrared photometry of planetary nebulae has been reported in the literature by several authors (Willner *et al.* 1972; Allen 1973; Persson and Frogel 1973; Cohen and Barlow 1974; Whitelock 1985; Kwok *et al.* 1986). Persson and Frogel pointed out that high density planetary nebulae ( $N_e > 10^4 \text{ cm}^{-3}$ ) usually show large excesses in  $K$  and  $L$  relative to the expected values for an ionized plasma continuum. This excess increases towards greater  $\lambda$ 's and usually has a maximum around  $\lambda \sim 30 \mu\text{m}$ . It has been interpreted as due to the presence of warm dust ( $T_d \sim 100 - 200 \text{ K}$ ) mixed with the ionized gas (Cohen and Barlow 1974; Pottasch *et al.* 1984).

We have started an extensive program to try to obtain a large sample of high density PN. We are interested in investigating a set of young, compact, high density planetary nebulae in order to establish their general characteristics that will help us understand better the infrared emission mechanisms and its evolution.

In this work we present JHK photometry for 31 planetary nebulae. Objects with small angular diameters ( $\phi < 10''$ ) have been preferentially selected and most of the reported high density nebulae have been included in the sample. A few slightly more extended objects were also observed.

## II. OBSERVATIONS

The observations were carried out during August 1985 and June 1986 with the infrared photometric system at the 2.1-m telescope of the Observatorio Astronómico Nacional in Baja California; a description of this system is given by Roth *et al.* (1984). All measurements were made with a 14" aperture and 30" beam separation in the N-S direction. Throw was adjusted in some cases in order to avoid contamination from nearby sources in the crowded regions. The photometry is referred to a net of standard stars from the list of Tapia *et al.* (1986).

From the comparison of our data with those objects previously reported (Willner *et al.* 1972; Persson and Frogel 1973; Whitelock 1985; Kwok *et al.* 1986) we find that in general there is good agreement in  $H$  and  $K$  measurements (within  $\pm 0.05$  mag); however, our measurements in the  $J$  band are systematically brighter than Whitelock's data by an excess of  $0.20 \pm 0.15$  mag. This difference is not expected to be due to our including extended emission, since our diaphragm is smaller and the effect is not present in  $H$  and  $K$  data; from the filter description (Glass 1973; Roth *et al.* 1984) it appears to be due to differences in the transmission of the  $J$  filter, in the sense that our filter is wider and includes a larger fraction of the  $\text{He}^+$  1.08  $\mu\text{m}$  feature.

In Table 1 the measured  $J$ ,  $H$  and  $K$  magnitudes are presented. In this table we also include the reddening value, electron density, radio flux at 5 GHz and  $\text{He}^+$  ionic abundance, as presented in the compilation by Pottasch (1984, Appendix 1 and Table III-12) except where specifically noted otherwise.

### III. DISCUSSION

In Figure 1 we present the intrinsic color-color diagram. The unreddened colors  $(J-H)_0$  and  $(H-K)_0$  have been determined by applying the reddening corrections:  $J_0 = J - 0.75 E(B-V)$ ,  $H_0 = H - 0.43 E(B-V)$ ,  $K_0 = K - 0.268 E(B-V)$  as derived by Glass and Feast (1982), and the color excesses listed in Table 1. The mean color of the sample (excluding BD+30°3639) is  $(J-H)_0 = -0.51$  and  $(H-K)_0 = +0.68$ . As pointed out by Whitelock (1985), the PN fall in a box around the mean colors and this area of the diagram is entirely different from the areas where other type of objects fall. Also indicated in the diagram is the location of the main sequence stars and

Table 1.  $JHK$  Photometry and Related Data for Planetary Nebulae

PK	Name	J	H	K	E(B-V)	log Ne	log F(5 GHz)	He <sup>+</sup> /H <sup>+</sup>	Notes
161-14 1	IC 2003	12.35 $\pm$ 0.08	12.49 $\pm$ 0.05	11.68 $\pm$ 0.04	0.12	3.83	1.63	0.048	e
190-17 1	J320	12.45 $\pm$ 0.06	13.05 $\pm$ 0.10	12.53 $\pm$ 0.10	0.21	3.94	1.49	0.108	
215-24 1	IC 418	8.17 $\pm$ 0.10	8.40 $\pm$ 0.08	7.58 $\pm$ 0.08	0.18	4.15	3.19	0.076	b,e
166+10 1	IC 2149	10.20 $\pm$ 0.05	10.46 $\pm$ 0.03	9.90 $\pm$ 0.02	0.19	3.60	2.45	0.071	e
221-12 1	IC 2165	10.69 $\pm$ 0.05	11.12 $\pm$ 0.04	10.35 $\pm$ 0.02	0.42	3.70	2.27	0.096	e
234+ 2 1	NGC 2440	10.67 $\pm$ 0.04	10.75 $\pm$ 0.04	10.07 $\pm$ 0.05	0.30	3.40	2.61	0.089	b
342+27 1	Me 2-1	12.76 $\pm$ 0.05	12.90 $\pm$ 0.05	12.25 $\pm$ 0.10	0.15	3.15	1.57	0.030	
25+40 1	IC 4593	10.63 $\pm$ 0.05	10.94 $\pm$ 0.05	10.53 $\pm$ 0.06	0.09	3.23	1.99	0.095	
13+32 1	Sn 1	13.31 $\pm$ 0.10	13.93 $\pm$ 0.15	13.26 $\pm$ 0.14	...	...	...	...	
43+37 1	NGC 6210	9.79 $\pm$ 0.05	10.40 $\pm$ 0.03	9.86 $\pm$ 0.02	0.06	3.88	2.41	0.100	
0+12 1	IC 4634	10.57 $\pm$ 0.08	11.25 $\pm$ 0.07	10.52 $\pm$ 0.07	0.35	3.75	2.15	0.099	
349+ 1 1	NGC 6302	9.00 $\pm$ 0.06	9.30 $\pm$ 0.04	8.18 $\pm$ 0.08	0.93	3.80	3.54	0.115	b,c
9+14 1	NGC 6309	11.60 $\pm$ 0.06	11.78 $\pm$ 0.04	10.97 $\pm$ 0.08	0.55	3.58	2.18	0.047	
2+ 5 1	NGC 6369	10.32 $\pm$ 0.06	10.38 $\pm$ 0.05	9.40 $\pm$ 0.08	1.40	3.44	3.29	...	b
96+29 1	NGC 6543	8.82 $\pm$ 0.02	9.50 $\pm$ 0.02	8.87 $\pm$ 0.05	0.07	3.60	2.93	0.111	
34+11 1	NGC 6572	8.06 $\pm$ 0.02	8.83 $\pm$ 0.03	8.08 $\pm$ 0.03	0.25	4.30	3.12	0.105	e
38+17 1	Cn 3-1	11.20 $\pm$ 0.05	11.38 $\pm$ 0.05	10.81 $\pm$ 0.05	0.32	3.85	1.87	0.040	
37- 6 1	NGC 6790	9.95 $\pm$ 0.05	10.37 $\pm$ 0.05	9.33 $\pm$ 0.05	0.56	4.17	2.43	0.101	c
45- 2 1	Vv 2-2	10.44 $\pm$ 0.05	10.83 $\pm$ 0.05	9.85 $\pm$ 0.05	0.94	5.47	2.34	0.130	c,d,e
64+ 5 1	BD+303639	8.90 $\pm$ 0.05	8.73 $\pm$ 0.05	7.77 $\pm$ 0.02	0.24	4.00	2.78	0.043	c
25-17 1	NGC 6818	10.90 $\pm$ 0.06	11.27 $\pm$ 0.03	10.81 $\pm$ 0.09	0.17	3.45	2.48	0.052	b
83+12 1	NGC 6826	9.94 $\pm$ 0.02	10.18 $\pm$ 0.05	9.80 $\pm$ 0.05	0.02	3.40	2.59	0.100	b
82+11 1	NGC 6833	11.76 $\pm$ 0.05	12.63 $\pm$ 0.05	11.90 $\pm$ 0.05	0.16	4.93	1.28	0.106	e
82+ 7 1	NGC 6884	10.62 $\pm$ 0.06	11.15 $\pm$ 0.03	10.29 $\pm$ 0.05	0.75	3.94	2.30	0.104	e
58-10 1	IC 4997	9.57 $\pm$ 0.03	10.41 $\pm$ 0.05	9.44 $\pm$ 0.05	0.34	5.30	2.10	0.130	c
89+ 0 1	NGC 7026	10.56 $\pm$ 0.10	10.86 $\pm$ 0.10	10.00 $\pm$ 0.06	0.83	3.98	2.41	0.098	
84- 3 1	NGC 7027	7.44 $\pm$ 0.05	7.47 $\pm$ 0.05	6.47 $\pm$ 0.06	0.93	4.90	3.80	0.076	c,e
86- 8 1	Hu 1-2	11.37 $\pm$ 0.04	11.76 $\pm$ 0.03	11.18 $\pm$ 0.02	0.42	3.95	2.19	0.075	
100- 5 1	IC 5217	11.75 $\pm$ 0.08	12.29 $\pm$ 0.08	11.51 $\pm$ 0.05	0.31	4.00	2.21	0.081	e
106-17 1	NGC 7662	10.29 $\pm$ 0.05	10.65 $\pm$ 0.08	9.95 $\pm$ 0.05	0.11	3.65	2.78	0.056	e
111- 2 1	Hb 12	9.46 $\pm$ 0.07	9.71 $\pm$ 0.08	8.66 $\pm$ 0.06	1.10	5.60	2.48	0.104	d

a. from Pottasch (1984)

b.  $\theta > 14''$

c. molecular or neutral envelope detected

d. radio flux at a higher frequency, nebula optically thick at 5 GHz

e.  $\text{He}^+/\text{H}^+$  from Torres-Peimbert and Peimbert (1977)

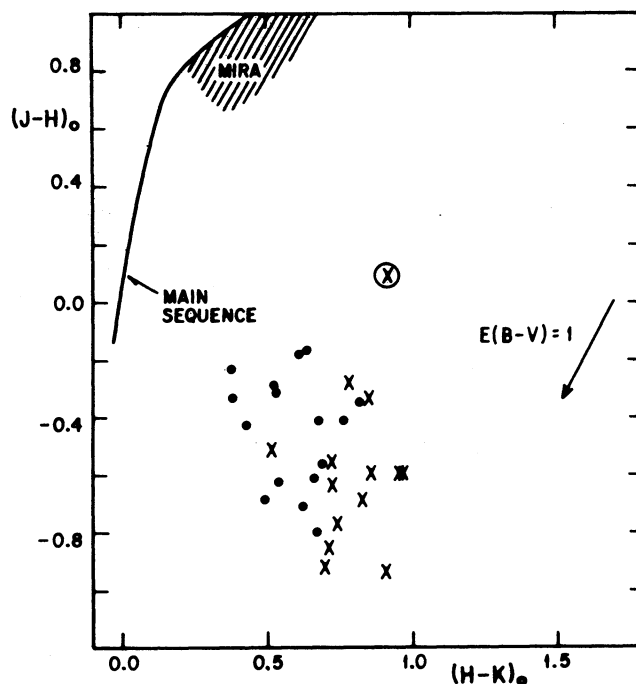


Fig. 1. Dereddened color-color diagram for the observed objects. Crosses are high density PN; filled circles, low density PN; circled cross is BD +30°3639.

Mira variables. We find that the high density planetary nebulae have a larger  $(H-K)$  value; the mean value is  $\langle (H-K)_0 \rangle = -0.8$ . In what follows we define "high" density planetary nebulae as those of  $N_e \geq 8 \times 10^3 \text{ cm}^{-3}$ , and "low" density ones, those of  $N_e < 8 \times 10^3 \text{ cm}^{-3}$ .

In Figure 2 the infrared magnitudes are compared with the radio fluxes at 5 GHz from Milne and Aller (1975) and Milne (1979), where the infrared to radio emission for a thermal gas is also shown. In this diagram, objects more extended than 14" are indicated with a horizontal arrow and IC 4997 is shown with a vertical arrow to indicate that it is optically thick at 5 GHz. In  $H$  and  $K$  all nebulae follow the predicted curve; however, most of high density nebulae show a systematic infrared excess; this effect is more noticeable in  $K$ . In the  $J$  filter, by contrast, all objects have excess infrared emission; it has been suggested (Whitelock 1985) that this excess is due to the  $\text{He}^+$  ( $2^3P - 2^3S$ ) line at  $1.08 \mu\text{m}$  which is the strongest emission line within the  $J$  band. This suggestion is confirmed in Figure 3, where we show the comparison  $(J-H)_0$  with  $\text{He}^+$  ionic abundance; there is a strong correlation in  $(J-H)_0$  with  $\text{He}^+/\text{H}^+$  for those objects that do not present excess in the  $H$  band. The  $1.08 \mu\text{m}$  line is produced not only by recombination but it is strongly affected by collisional excitation from the metastable  $2^3S$  level, but its effective collisional excitation rate is only weakly dependent on the electron temperature. The strong correlation between the  $\text{He}^+$  abundance and the  $2^3S$  population causes the correlation of the line intensity at  $1.08 \mu\text{m}$  and  $\text{He}^+$  abundance (Osterbrock 1974; Berrington *et al.* 1985).

In Figure 4 we show the comparison of the colors  $(J-H)_0$  and  $(H-K)_0$  with electron density for each object. We have marked the mean color values from our data. In the  $(J-H)_0$  vs  $\log N_e$  diagram a negative slope is apparent for most of the objects. This behavior is consistent with the fact that the  $\text{He}^+$   $1.08 \mu\text{m}$  emission is produced principally by collisional excitation and increases with optical depth (Osterbrock 1974). The few objects outside this correlation are high density nebulae and show strong near infrared excess (BD+30°3639, IC 418, NGC 7027 and Hb-12) or an anomalously low  $1.08 \mu\text{m}$  emission line like BD+30°3639 (Vaughan 1968), probably due to dust absorption of the line (Persson 1972). Dust absorption could also be affecting the  $1.08 \mu\text{m}$  line intensity in the other high density objects.

In the  $(H-K)_0$  versus  $\log N_e$  diagram low density objects lie about the expected value for a  $10^4 \text{ K}$  plasma, (of 0.7), while most of the high density objects show a color excess

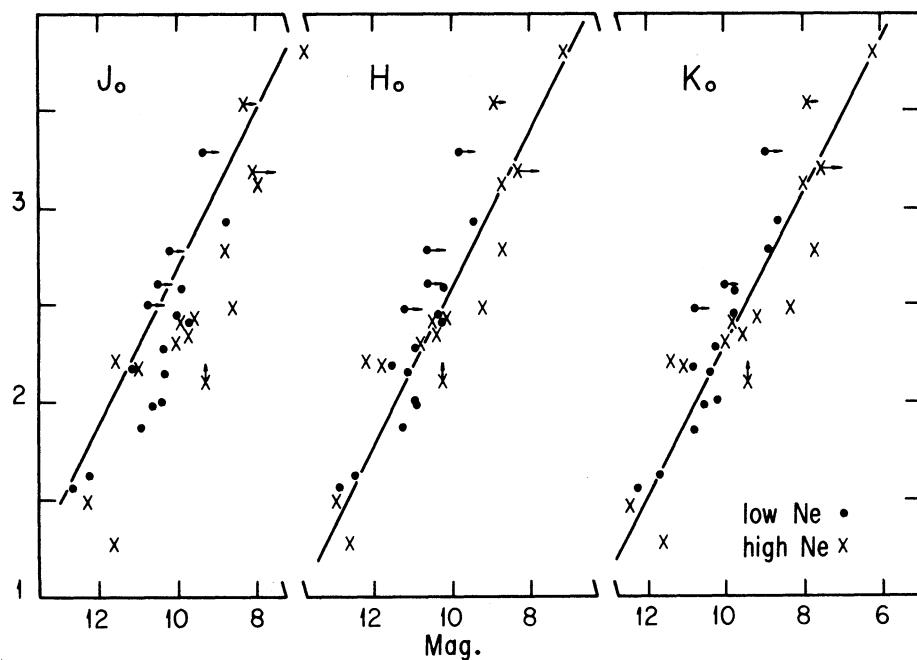


Fig. 2. Radio fluxes versus dereddened infrared magnitudes. 5 GHz fluxes from Milne and Aller (1975) and Milne (1979). Symbols are the same as in Figure 1. Horizontal arrows are attached to nebulae larger than 14" diameter. A vertical arrow is attached to IC 4997 which is optically thick at 5 GHz. Solid lines correspond to the theoretical relationship for  $10^4$  K ionized plasma.

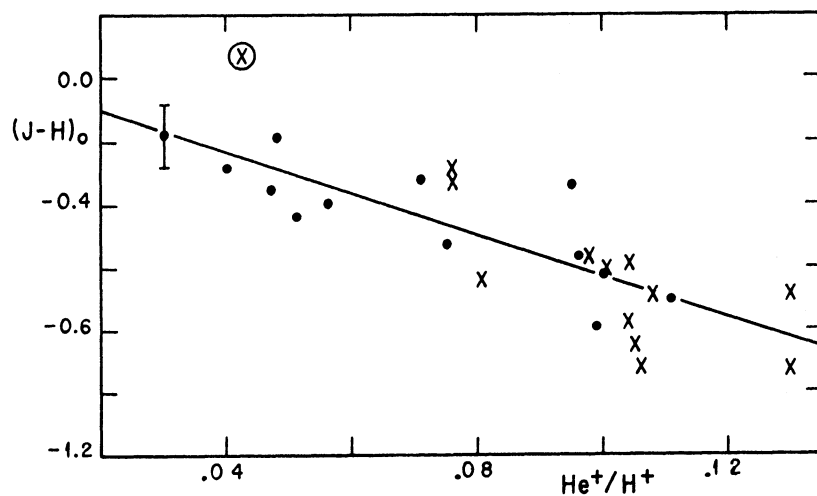


Fig. 3.  $(J-H)_0$  dereddened index versus  $\text{He}^+$  ionic abundance. The extended PN have been omitted (PN > 14") because of stratification effects. Symbols are the same as in Figure 1. The line represents the best fit.

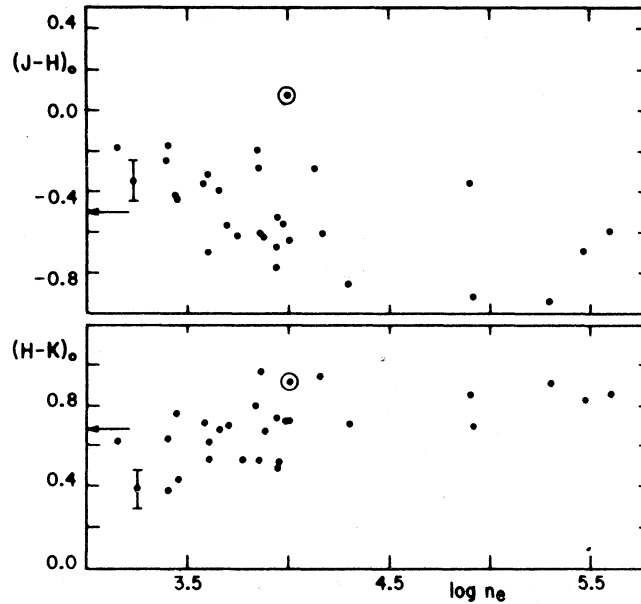


Fig. 4. Dereddened color indices versus density. Circled point corresponds to BD +30°3639. The arrows show the mean colors of the sample.

with a mean  $(H-K)_0$  value of about 0.8. As it was said before most PN show far infrared excess. The detection of this excess at  $2.2 \mu\text{m}$  for the densest nebulae seems to indicate that these objects have higher dust temperatures than low density nebulae. Similar results have been obtained from IRAS observations by Pottasch *et al.* (1984) and Kwok *et al.* (1986) who also suggest that one of the dust heating mechanisms for the youngest planetary nebulae is direct starlight which becomes less efficient for low density extended objects due to geometrical dilution.

#### IV. CONCLUSIONS

From the JHK photometry for 31 planetary nebulae we find:

- 1) In the color-color diagram the planetary nebulae are grouped in an area about  $(J-H)_0 = -0.51$  and  $(H-K)_0 = +0.68$ .
- 2) High density nebulae have an excess in the mean value of  $(H-K)_0$  over low density objects.
- 3) Most high density nebulae show an infrared excess in H and K filters over the expected free-free emission that is not present in low density objects. This excess is interpreted as due to warm dust in the high density (younger) objects.
- 4) The PN in our sample show a correlation of  $(J-H)_0$  with  $\text{He}^+$  ionic abundance; this is due to the J filter response that allow a large fraction of the  $1.08 \mu\text{m}$   $\text{He}^+$  line, and the proportionality between the  $1.08 \mu\text{m}$  line intensity and the  $\text{He}^+$  abundance.

The authors gratefully acknowledge the assistance of M. Roth, M. Tapia, and the staff of the Observatorio Astronómico Nacional during observations and data reduction, also fruitful discussions with M. Peimbert.

#### REFERENCES

- Allen, D.A. 1973, *M.N.R.A.S.*, **161**, 145.  
 Aitken, D.K. and Roche, P.F. 1982, *M.N.R.A.S.*, **200**, 217.  
 Berrington, K.A., Burke, P.G., Freitas, L.C.G., and Kingston, A.E. 1985, *J. Phys. B: At. Mol. Phys.*, **18**, 4135.  
 Cohen, M. and Barlow, M.J. 1974, *Ap. J.*, **193**, 401.

- Glass, I.S. and Feast, M.W. 1982, *M.N.R.A.S.*, 198, 199.
- Glass, I.S. 1973, *M.N.R.A.S.*, 164, 155.
- Kwok, S., Hrivnak, B.J., and Milone, E.F. 1986, *Ap. J.*, 303, 451.
- Milne, D.K. 1979, *Astr. and Ap., Suppl.*, 36, 227.
- Milne, D.K. and Aller, L.H. 1975, *Astr. and Ap.*, 38, 183.
- Osterbrock, D.E. 1974, *Astrophysics of Gaseous Nebulae*, (W.H. Freeman and Co.: San Francisco).
- Persson, S.E. 1972, Ph. D. dissertation, California Institute of Technology.
- Persson, S.E. and Frogel, J.A. 1973, *Ap. J.*, 182, 503.
- Pottasch, S.R. 1984, *Planetary Nebulae*, (
- Pottasch, S.R., Baud, B., Beintema, D., Emerson, J., Habing, H.J., Harris, S., Houck, J., Tenningo, R., and Marsden, P. 1984, *Astr. and Ap.*, 138, 10.
- Rodríguez, L.F. 1987, in *Planetary and Proto-Planetary Nebulae. From IRAS to ISO*, Ed. A. Preite-Martinez, (D. Reidel: Dordrecht), in presss.
- Roth, M., Iriarte, A., Tapia, M., and Resendiz, G. 1984, *Rev. Mexicana Astron. Astrof.*, 9, 25.
- Tapia, M., Neri, L., and Roth, M. 1986, *Rev. Mexicana Astron. Astrof.*, 13, 115.
- Torres-Peimbert, S. and Peimbert, M. 1977, *Rev. Mexicana Astron. Astrof.*, 2, 181.
- Vaughan Jr., A.H. 1968, *Ap. J.*, 154, 87.
- Whitelock, P.A. 1985, *M.N.R.A.S.*, 213, 59.
- Willner, S.P., Becklin, E.E., Visvanathan, N. 1972, *Ap. J.*, 175, 699.

Miriam Peña and Silvia Torres-Peimbert: Instituto de Astronomía, UNAM, Apartado Postal 70-264, 04510 México, D.F., México.